



# CHORUS

This is the accepted manuscript made available via CHORUS. The article has been published as:

## Two and three nucleons in a trap, and the continuum limit

J. Rotureau, I. Stetcu, B. R. Barrett, and U. van Kolck

Phys. Rev. C **85**, 034003 — Published 14 March 2012

DOI: [10.1103/PhysRevC.85.034003](https://doi.org/10.1103/PhysRevC.85.034003)

# Two and Three Nucleons in a Trap and the Continuum Limit

J. Rotureau,<sup>1,2</sup> I. Stetcu,<sup>3,4</sup> B.R. Barrett,<sup>2</sup> and U. van Kolck<sup>2</sup>

<sup>1</sup>*Fundamental Physics, Chalmers University of Technology, 412 96 Göteborg, Sweden*

<sup>2</sup>*Department of Physics, University of Arizona, Tucson, AZ 85721, USA*

<sup>3</sup>*Department of Physics, University of Washington,  
Box 351560, Seattle, WA 98195-1560, USA*

<sup>4</sup>*Theoretical Division, Los Alamos National Laboratory,  
Los Alamos, New Mexico 87545, USA*

## Abstract

We describe systems of two and three nucleons trapped in a harmonic-oscillator potential with interactions from the pionless effective field theory up to next-to-leading order (NLO). We construct the two-nucleon interaction using two-nucleon scattering information. We calculate the trapped levels in the three-nucleon system with isospin  $T = 1/2$  and determine the three-nucleon force needed for stability of the triton. We extract neutron-deuteron phase shifts, and show that the quartet scattering length is in good agreement with experimental data.

PACS numbers:

Keywords:

## I. INTRODUCTION

A major goal of nuclear physics is to derive nuclear structure “*ab initio*”, that is, starting from inter-nucleon interactions consistent with QCD. This requires a many-body technique that provides a numerical solution to the Schrödinger equation for a system of  $A$  interacting particles within a restricted space, which is sufficiently small to be handled by accessible computers. The no-core shell model (NCSM) [1] is such a many-body technique, where the restricted space is generated by harmonic-oscillator (HO) wavefunctions. In the traditional NCSM, effective inter-nucleon interactions adapted to the restricted space are derived from a given potential.

The inter-nucleon potential is not directly observable; it is merely an intermediate step to obtain measurable quantities. Its very definition requires the choice of a restricted space, and care is needed to make sure that measurable quantities are independent of this choice, that is, are renormalization-group (RG) invariant. The framework to accomplish this is effective field theory (EFT). A potential constructed in EFT is improvable in a systematic expansion, and can be used as input in many-body problems. Some of current *ab initio* calculations do, indeed, start with a potential inspired by EFT, but they suffer from limited (or no) RG invariance. Alternatively, we can construct manifestly RG-invariant observables starting from inter-particle interactions defined directly within the restricted space of the many-body technique using the general principles of EFTs [2, 3]. In Ref. [2], we have demonstrated this idea for a NCSM-type restricted space in leading order (LO) of the so-called pionless EFT.

At low energies, the physics of two- and few-body systems is insensitive to the details of the interaction at short distances. Thus, in the case of an interaction of finite range  $R$ , short-range details are irrelevant for the description of processes involving momenta  $k \lesssim 1/R$ . The pionless, or contact, EFT [4] uses this separation of scales to construct the potential as a sum of delta functions and their derivatives, which for observables translates into expansions in powers of  $kR$ . A particularly interesting class of systems is that where the two-body  $S$ -wave scattering length  $a_2$  is large,  $a_2 \gg R$ , because then the LO potential solved exactly produces a real or virtual bound state at  $k \simeq i/a_2$ . This EFT has been applied to nuclear physics [5–8], where  $a_2 \gg 1/m_\pi$ , the inverse of the pion mass. At larger momentum,  $k \sim m_\pi$ , pions need to be taken into account, and the more sophisticated pionful, or chiral, EFT [4] is needed where, in addition to delta functions, pion exchange is explicitly included.

The definition of the delta functions themselves is tied to the restricted space. Their strengths depend on the size of the space. Fitting the strengths of the two- and three-nucleon contact interactions that appear at LO in the pionless EFT to reproduce the deuteron, triton and  ${}^4\text{He}$  ground-state binding energies, the energies of other  ${}^4\text{He}$  and  ${}^6\text{Li}$  states were found in Ref. [2] to agree with experiment within the expected errors for a LO calculation ( $\sim 30\%$ ).

In order to demonstrate systematic improvement, one needs to calculate corrections beyond LO. However, beyond LO the number of couplings in the EFT expansion increases significantly, making the fit to few-body binding energies impractical. Hence, we have developed an approach that requires only information from the two-nucleon system in order to fix the two-nucleon interactions. This can be done by considering the two-body system in a HO potential and relating the energy levels to the scattering parameters. In Refs. [9, 10] we have constructed the two-body interaction up to next-to-next-to-leading order (NNLO), which reproduces the lowest energy levels obtained from given scattering parameters. We have used it to calculate the spectra of trapped systems of a few two-state fermions [9, 11],

while systems of bosons were addressed in Ref. [12].

We have also suggested [3] that the same method can be used for nucleons. Here we implement this approach. In fact, one of the goals of this paper is to show that meaningful results can be obtained for nuclear physics by trapping the nuclear system. This is not surprising, since in the middle of the trap the wavefunction has no knowledge of the trap's existence [10]. However, while in atomic systems the trap is physical and dominates the long-range behavior, for nuclear systems the trap is just an artifact introduced in order to define the interaction. We therefore need an extra step at the end, that of making the trap large, in order to extrapolate energies to the “continuum” limit. The discrete states in the trap approach the untrapped spectrum of a few bound states and a continuum of scattering states. Following the procedure devised in Ref. [11] for the atom-dimer system, we extract the neutron-deuteron scattering length from the trapped-system levels at NLO. This extends to the three-nucleon system the “inverse” connection between trapped levels and scattering stressed at the two-body level in Refs. [10, 13].

A significant complication of the nuclear case, compared to the two-state-fermion case, is the role of three-body forces. In the absence of the trap, a three-nucleon force is needed in the pionless EFT at LO in order to achieve RG invariance [7]. The same is true for bosons [14], and it has been shown in Ref. [12] that this feature is not affected by the presence of the trap, as expected from the short-distance character of renormalization. We show here that the same holds for nucleons in the presence of the trap, and determine the three-nucleon force needed for cutoff independence up to NLO.

The paper is organized as follows. After we set up our framework in Sec. II, we construct in Sec. III the two-nucleon interaction up to NLO using the two-nucleon scattering data as input. In Sec. IV we apply the formalism to three nucleons in two different channels described by total isospin  $T = 1/2$  and total angular momentum/parity: (i)  $J^\pi = 3/2^+$ , which is similar to the system of three two-component fermions and does not involve a three-body force up to NLO; and (ii)  $J^\pi = 1/2^+$ , which requires a contact three-body force already in LO. In the first channel, we calculate the quartet scattering length for deuteron-nucleon scattering, obtaining the same accuracy as similar continuum calculations, while for the second channel we demonstrate the collapse of the system, as in free space. We summarize and conclude in Sec. V.

## II. PRELIMINARIES

We consider a non-relativistic system of  $A$  nucleons of mass  $m_N$  trapped in a HO potential of frequency  $\omega$ , or alternatively of length

$$b = \sqrt{\frac{2}{m_N \omega}}. \quad (1)$$

The HO potential can be decomposed into two pieces, one acting on the center of mass (CM) of the particles and one on their relative coordinates. We denote by  $\vec{r}_i$  ( $\vec{p}_i$ ) the position (momentum) of particle  $i$  with respect to the origin of the HO potential. The Hamiltonian describing the relative motion of the particles is given by

$$H = H_0 + \sum_{i < j} V_{ij} + \sum_{i < j < k} V_{ijk} + \dots, \quad (2)$$

with

$$H_0 = \frac{\omega}{2A} \sum_{i < j} \left[ \frac{b^2}{2} (\vec{p}_i - \vec{p}_j)^2 + \frac{2}{b^2} (\vec{r}_i - \vec{r}_j)^2 \right]. \quad (3)$$

Here  $V_{ij}$  and  $V_{ijk}$  denote the two-nucleon and three-nucleon potentials, respectively, more-body interactions being lumped into “...”.

In pionless EFT, the inter-nucleon potential is expanded in derivatives of delta functions, or powers of momenta in momentum space. An important task in EFT is to provide a power counting for observables. One can show [5–8] that in pionless EFT observables can be written as expansions in  $Q/M_{hi}$ , where  $Q$  denotes the generic external momenta of the process under consideration and  $M_{hi} \sim m_\pi$  is the scale at which pion effects need to be accounted for explicitly. At any order of truncation, errors scale as  $Q/M_{hi}$  to the power of the most important neglected order. Of course, as in any theory one has to carry out renormalization. Delta functions are singular and require an ultraviolet (UV) momentum cutoff  $\Lambda_A$  in order for them to be well defined. Observables are (nearly) independent of the arbitrary cutoff as long as the coefficients of the delta functions depend on the UV cutoff appropriately —and as long as there are enough interactions at the given order, which is a non-trivial consistency check on the power counting. The truncation generates an error due to the cutoff that grows as  $Q/\Lambda_A$ , so cutoff errors are minimized as  $\Lambda_A$  increases. However, one should keep in mind that there are always errors that grow as  $Q/M_{hi}$ , which cannot be minimized by increasing the cutoff.

For convenience we diagonalize  $H$  using HO wavefunctions. We can work with Jacobi coordinates defined in terms of differences between the CM positions of sub-clusters within the  $A$ -body system, e.g.,

$$\begin{aligned} \vec{\xi}_1 &= \sqrt{\frac{1}{2}} (\vec{r}_1 - \vec{r}_2), \\ \vec{\xi}_2 &= \sqrt{\frac{2}{3}} \left[ \frac{1}{2} (\vec{r}_1 + \vec{r}_2) - \vec{r}_3 \right], \\ &\vdots \\ \vec{\xi}_{A-1} &= \sqrt{\frac{A-1}{A}} \left[ \frac{1}{A-1} (\vec{r}_1 + \vec{r}_2 + \cdots + \vec{r}_{A-1}) - \vec{r}_A \right]. \end{aligned} \quad (4)$$

In terms of them, the HO Hamiltonian (3) becomes a collection of  $A - 1$  HOs,

$$H_0 = \frac{\omega}{2} \sum_{\rho=1}^{A-1} \left[ \left( \frac{b \vec{p}_{\xi_\rho}}{\sqrt{2}} \right)^2 + \left( \frac{\sqrt{2} \vec{\xi}_\rho}{b} \right)^2 \right], \quad (5)$$

where  $\vec{p}_{\xi_\rho}$  is the momentum canonically conjugated to  $\vec{\xi}_\rho$ . We use a basis made out of properly antisymmetrized combinations of  $A - 1$  eigenfunctions  $\phi_{n_i l_i}$  of  $H_0$ , which are characterized by the radial quantum numbers  $n_i$  and the angular momenta  $l_i$ . The energy of a basis state can be written as  $[N_A + 3(A - 1)/2]\omega$ , with  $N_A$  an integer,

$$N_A = \sum_{i=1}^{A-1} (2n_i + l_i). \quad (6)$$

A numerical calculation can only be carried out with a finite number of basis elements, which span the “model space”. We include in the model space all states up to a maximum integer  $N_A^{max}$ , which provides a natural momentum cutoff [2]

$$\Lambda_A = \frac{1}{b} \sqrt{2N_A^{max} + 3(A - 1)}. \quad (7)$$

Since there is a minimum step in energy supplied by  $\omega$ , one can think of the model space as containing also an infrared (IR) cutoff [2]

$$\lambda = \frac{1}{b}. \quad (8)$$

Within the low energies where the EFT applies, the errors introduced by the limited size of the model space should decrease as  $\lambda$  decreases, as well as  $\Lambda_A$  increases. This is the simple requirement that the HO oscillator be wide enough to accommodate the nuclear states we are interested in.

As the trap is made larger, the states after diagonalization will approach their untrapped counterparts. The lowest states become the free-nucleus bound states, while states higher up in energy coalesce into a continuum of scattering states. Conversely, sufficiently near the center of a given trap wavefunctions resemble those of the untrapped system. Yet, they must also depend on the corresponding energy. Thus, there is a connection between the energy levels in the trap and the parameters that characterize the untrapped wavefunctions. The latter are related to the scattering, or  $T$ , matrix, and thus to phase shifts, which at sufficiently low energies can be described by effective-range expansion (ERE) parameters [15]. Thus, there is a relation between trap levels and phase shifts, which we can explore in two ways. First, we can use the scattering data as input to determine the levels inside the trap, and use a subset of the latter to fix the coefficients of the inter-nucleon interactions [9, 10]. Other levels, at the same  $A$  or not, can then be predicted. Second, the predicted levels can be used to calculate scattering phase shifts [10, 11].

In the remainder of the paper we carry out this method explicitly to NLO in the pionless EFT for  $A = 2, 3$ . We use the known two-nucleon ERE parameters to determine the two-nucleon interaction, and then extract neutron-deuteron scattering information. In this first approach we do not include electromagnetic interactions nor isospin-breaking effects, which are of higher order. The same method to deal with nuclear systems can in the future be carried out with the pionful EFT [4], where  $M_{hi}$  is higher and, consequently, denser systems can be handled.

### III. TWO NUCLEONS IN A HARMONIC TRAP

We construct a two-body potential based on the ideas of EFT to describe the interaction between the two nucleons. The method is described in more detail for a single channel in Ref. [10].

The two-nucleon interaction can be expanded as

$$V(\vec{\xi}_1) = \frac{C_0}{2\sqrt{2}} \delta(\vec{\xi}_1) - \frac{C_2}{4\sqrt{2}} \left[ (\nabla^2 \delta(\vec{\xi}_1)) + \delta(\vec{\xi}_1) \nabla^2 \right] + \dots, \quad (9)$$

where  $C_0$  and  $C_2$  are parameters, and “...” denote terms of higher orders. At LO, the Schrödinger equation of the trapped two-nucleon system is solved exactly with the potential

given by the first term in the expression (9). For a given ultraviolet cutoff  $\Lambda_2$ , the low-energy constant  $C_0(\Lambda_2)$  is adjusted such that one energy level of the two-nucleon system, which we take to be the lowest, is reproduced for all values of  $\Lambda_2$ . Corrections beyond leading orders should be calculated in increasing orders in perturbation theory. At NLO, in particular, corrections are obtained by considering the second term in Eq. (9) in first-order perturbation theory, with  $C_0(\Lambda_2)$  and  $C_2(\Lambda_2)$  adjusted to reproduce two two-nucleon levels, here the lowest two. Because the second term contributes to the ground state, the  $\Lambda_2$  dependence of  $C_0$  changes. It is convenient to write  $C_0(\Lambda_2) = C_0^{(0)}(\Lambda_2) + C_0^{(1)}(\Lambda_2) + \dots$  and  $C_2(\Lambda_2) = C_2^{(1)}(\Lambda_2) + \dots$ , where the superscript  $(n)$  corresponds to the  $\Lambda_2$  dependence fixed at N $^{(n)}$ LO. Only the  $C_0^{(0)}(\Lambda_2)$  piece of the interaction is iterated to all orders.

The interactions up to NLO affect only  $S$  waves, higher waves coming at NNLO and beyond. Differently from the case of two-component fermions, in the case of two nucleons there are two  $L = 0$  channels to consider, where the nucleons couple to total spin  $S = 0, 1$ . For a relative momentum  $k \ll m_\pi$  the interaction in free space, *i.e.* when there is no trap, gives rise [5] to a phase shift  $\delta_2(k)$  given by the ERE [15],

$$k \cot \delta_2(k) = -\frac{1}{a_2} + \frac{r_2}{2}k^2 + \dots, \quad (10)$$

where  $a_2, r_2, \dots$  are, respectively, the scattering length, effective range, and higher ERE parameters not shown explicitly. The ERE parameters can be directly related [5] to the parameters in Eq. (9). At LO, we obtain only the scattering-length term, while at NLO the effective-range term appears as well. In the following, we use the empirical values  $a_{2t} = 5.425$  fm and  $r_{2t} = 1.749$  fm in the triplet channel, and  $a_{2s} = -18.7$  fm and  $r_{2s} = 2.75$  fm in the singlet channel [16]. Bound states can be obtained by calculating the position of the pole of the  $T$  matrix in each channel,

$$k \cot \delta_2(k) = -ik. \quad (11)$$

In the triplet (singlet) channel the positive (negative) scattering length signals a real (virtual) bound state. At NLO in free space the deuteron energy is  $E_d^{free} = -2.213$  MeV.

When two nucleons are confined within the harmonic trap, we diagonalize the Hamiltonian (2) for  $A = 2$  with the potential (9) in the basis of HO wavefunctions  $\phi_{nl}(\vec{\xi}_1)$ . The unperturbed levels are characterized by  $N_2 = 2n + l$ . Since to NLO the inter-nucleon potential is purely  $S$ -wave, levels with  $l \geq 1$  are unaffected by it. The  $S$ -wave energies  $E_{2,n}$ , on the other hand, depend on the EFT parameters and thus on the phase shifts. These energies are solutions of the transcendental equation

$$\frac{\Gamma(3/4 - E_{2;n}/2\omega)}{\Gamma(1/4 - E_{2;n}/2\omega)} = -\sqrt{E_{2;n}/2\omega} \cot \delta_2 \left( \sqrt{m_N E_{2;n}} \right), \quad (12)$$

where  $\delta_2(k)$  is given by Eq. (10). Equation (12) was first obtained [17] by solving the Schrödinger equation using a pseudopotential [18], but it can be derived directly within the EFT framework [10] (see also Ref. [19]). As in the absence of the trap, at LO the right-hand side contains only the scattering-length term, while at NLO the effective-range term appears as well.

As an illustration, we consider the “deuteron in the trap”, that is, the lowest state in the trap which goes into the deuteron as  $b \gg a_{2t}$ . Figure 1 shows the lowest energy  $E_d$  of two nucleons in the triplet configuration as a function of the frequency  $\omega$ . The energy  $E_d$  is obtained by solving Eq. (12). At NLO,  $E_d = -2.123$  MeV for  $\omega = 1$  MeV, and  $E_d = -2.212$



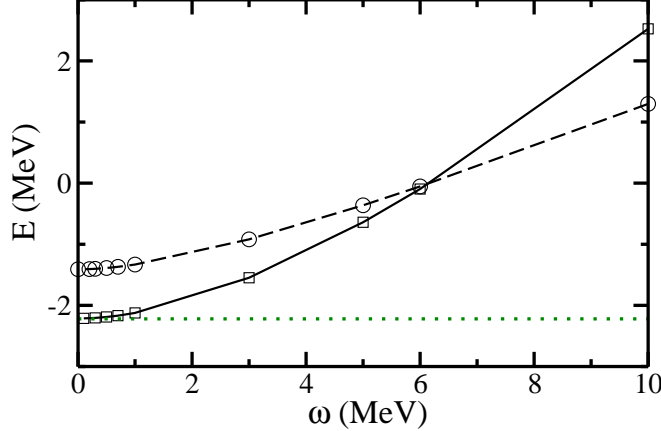


FIG. 1: Ground-state energy of the trapped two-nucleon system in the  ${}^3S_1$  channel (deuteron in the trap) as a function of the frequency  $\omega$ . The energy at LO (NLO) is given by the dashed (solid) line. For small values of  $\omega$ , the energy converges to the value in free space, which is, at NLO, indicated by the dotted line.

MeV for  $\omega = 0.1$  MeV, in good agreement with the energy of the bound state in free space. Such a good agreement is not surprising, as for small  $\omega$  the corrections to the energy due to the trap scale in LO with  $(a_{2t}/b)^4$  [13].

We use this and other energy levels given by Eq. (12) to determine the parameters  $C_0$ ,  $C_2$ , *etc.* In the triplet channel,  $C_0^{(0)}(\Lambda_2)$  is found by demanding that it produces the LO deuteron in the trap. In Fig. 2 we show the running of the triplet coupling constant  $\Lambda_2 C_0^{(0)}(\Lambda_2) m_N$  as a function of the cutoff  $\Lambda_2$ , for  $\omega = 1$  MeV. For large  $\Lambda_2$ ,  $C_0^{(0)}(\Lambda_2) \rightarrow -2\pi^2(m_N \Lambda_2)^{-1}$ . At NLO,  $C_0^{(1)}(\Lambda_2)$  and  $C_2^{(1)}(\Lambda_2)$  are obtained from the NLO deuteron in the trap and the first excited-state solution of Eq. (12) considering both the scattering length  $a_{2t}$  and the effective range  $r_{2t}$ . In Fig. 3 we show the running of the triplet coupling constants  $C_0^{(1)}(\Lambda_2) m_N / r_{2t}$  and  $\Lambda_2^2 C_2^{(1)}(\Lambda_2) m_N / r_{2t}$  as a function of the cutoff  $\Lambda_2$ , again for  $\omega = 1$  MeV. For large enough  $\Lambda_2$ ,  $C_0^{(1)}(\Lambda_2)$  becomes constant and  $C_2^{(1)}(\Lambda_2) \propto \Lambda_2^{-2}$  [10]. The running of coupling constants is qualitatively similar for other frequencies. In the singlet channel we obtain analogous results using as input the corresponding scattering parameters.

Once the EFT couplings are determined from a couple of levels, the other levels can be calculated. They do not agree exactly with the levels of Eq. (12) at finite  $\Lambda_2$ , but approach them as  $\Lambda_2 \rightarrow \infty$ . In Fig. 4 we show the first excited state at LO and the second excited state at NLO as a function of the size of the model space characterized by  $N_2^{max}$ . As  $N_2^{max}$  increases the energies in the finite model space converge to the exact energies of Eq. (12). It is clear that convergence is sped up when the correction to the potential at NLO is included: the first excited state is now simply fitted, and the second excited state is very close to the exact value even at relatively small  $N_2^{max}$ .

As discussed in Ref. [10], with the calculated levels input to the left-hand side of Eq. (12) we can invert the procedure and obtain scattering phase shifts for a given cutoff. In Fig. 5, we plot the phase shifts for both triplet and singlet configurations, for  $\omega = 1$  MeV and  $N_{max} = 20$ . Also displayed are the corresponding ERE phase shifts and the Nijmegen neutron-proton ( $np$ ) phase-shift analysis (PSA) [20]. (The discrepancy observed in the  ${}^1S_0$



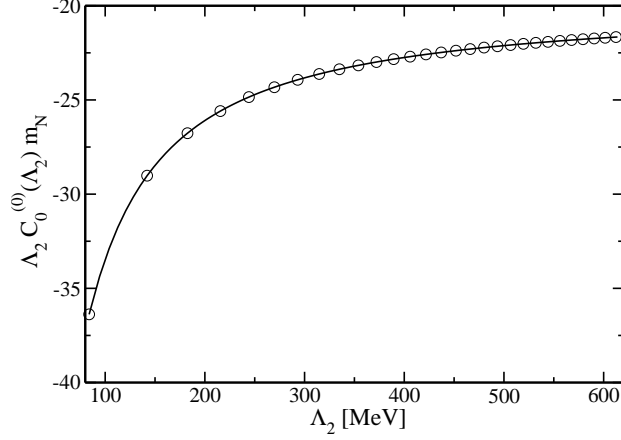


FIG. 2: LO two-nucleon coupling constant  $\Lambda_2 C_0^{(0)}(\Lambda_2) m_N$  in the  $^3S_1$  channel as a function of the cutoff  $\Lambda_2$ , for  $\omega = 1$  MeV.

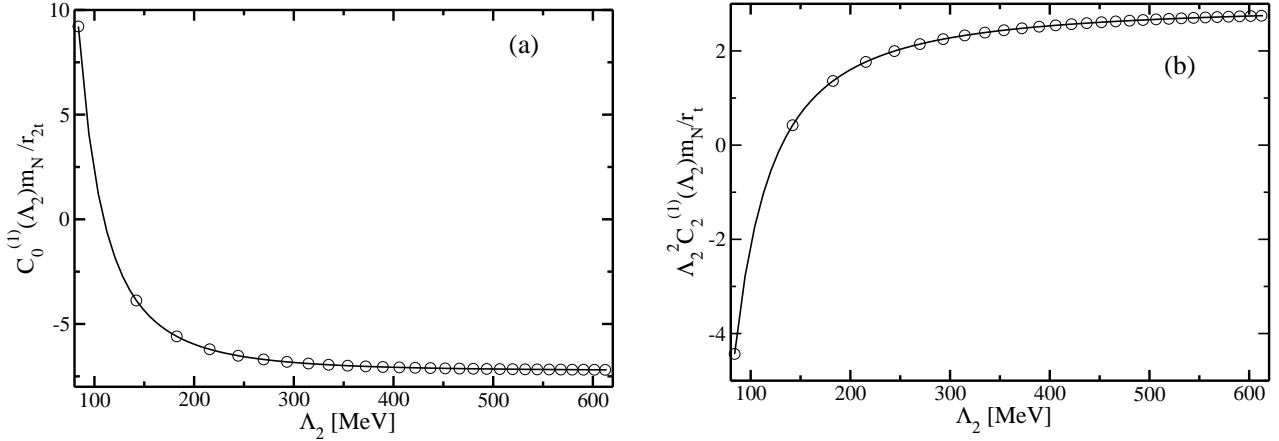


FIG. 3: NLO two-nucleon coupling constants in the  $^3S_1$  channel as a function of the cutoff  $\Lambda_2$ , for  $\omega = 1$  MeV: (a)  $C_0^{(1)}(\Lambda_2) m_N / r_{2t}$ ; (b)  $\Lambda_2^2 C_2^{(1)}(\Lambda_2) m_N / r_t$ .

channel between ERE and PSA phase shifts appears because the ERE is calculated with neutron-neutron scattering length and effective range. The difference is an isospin-breaking effect of higher order than what is considered here.) At low energies, as expected, one obtains good agreement with the ERE and with the Nijmegen PSA. Agreement worsens as one goes to higher and higher energies, since the higher energy levels show more effect of the finite cutoff, which effectively induces higher-order ERE terms. Better agreement with ERE is obtained as the cutoff increases, and, for a given cutoff, agreement improves systematically order by order, as long as the momentum of the state is well below the cutoff imposed by the model space (see Fig. 5 of Ref. [10]).

One can look at the phase shifts as predictions of the theory, but there are easier ways to carry out this two-nucleon calculation (see for example Ref. [5]). The motivation to use the HO basis comes from wanting to study larger systems. We now turn to the simplest such cases, the three-nucleon system.

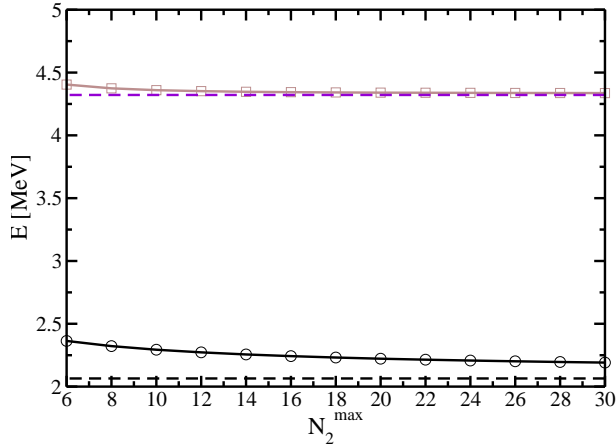


FIG. 4: (Color online) Energies of the first (circle) and second (square) excited states of the two-nucleon system in the  ${}^3S_1$  channel at LO and NLO, respectively, as function of  $N_2^{max}$ , for  $\omega = 1$  MeV. The dashed lines correspond to the exact solution given by Eq. (12).

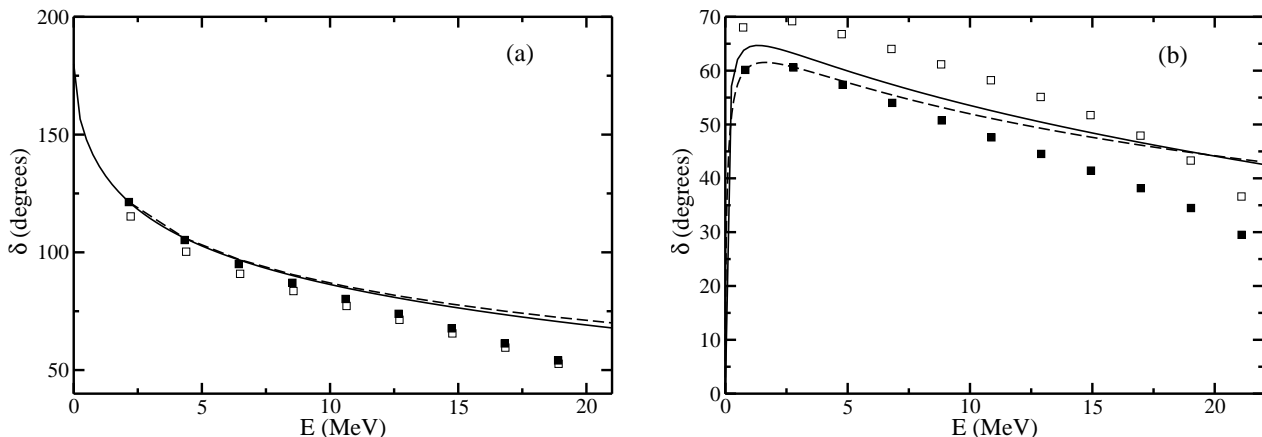


FIG. 5: Phase shifts for the two-nucleon system at  $\omega = 1$  MeV and  $N_{max} = 20$  as a function of the relative energy: (a)  ${}^3S_1$ ; (b)  ${}^1S_0$ . EFT results at LO (NLO) are marked by empty (filled) squares; the ERE up to the effective range is indicated by a dashed line; and the Nijmegen  $np$  PSA [20] by a solid line.

#### IV. THREE NUCLEONS IN A HARMONIC TRAP

We now consider a system of three nucleons trapped within an HO potential. The situation here involves elements encountered before in both the two-state-fermion [9, 11] and boson [12] cases.

Since no symmetry forbids a three-nucleon potential, we have to consider this additional element. In pionless EFT, the three-nucleon potential is also expressed in terms of delta functions,

$$V(\vec{\xi}_1, \vec{\xi}_2) = D_0 \delta(\vec{\xi}_1) \delta(\vec{\xi}_2) + \dots, \quad (13)$$

where  $D_0$  is a parameter and derivatives terms are buried in “...”. Just as the two-body parameters,  $D_0$  and other three-body parameters depend on the cutoff. In Ref. [7] it has been shown that in free space the non-derivative three-body force is needed for RG invariance

already at LO, while derivative corrections appear at NNLO and higher. The non-derivative  $D_0$  interaction contributes only when we place three nucleons at the origin in a relative  $S$  wave, that is, when the total isospin is  $T = 1/2$  and the total angular momentum and parity is  $J^\pi = 1/2^+$ . To NLO, we thus need information about one three-nucleon observable, such as the ground-state energy.

In the trap, we use the basis states

$$\mathcal{A} \left\{ \left[ \phi_{n_1 l_1}(\vec{\xi}_1) \otimes \phi_{n_2 l_2}(\vec{\xi}_2) \right]_L \left| \left( \frac{1}{2} \frac{1}{2} \right)_{s_2} \frac{1}{2}; S \right| \left( \frac{1}{2} \frac{1}{2} \right)_{t_2} \frac{1}{2}; T \right\}, \quad (14)$$

which have the spatial part constructed using HO wavefunctions in  $\vec{\xi}_1$  and  $\vec{\xi}_2$  with quantum numbers  $n_1, l_1$  and  $n_2, l_2$ , respectively, with the angular momentum coupled to  $L$ , while the spin (isospin) part is constructed by coupling first two spins (isospins)  $s = 1/2$  ( $t = 1/2$ ) into spin (isospin)  $s_2$  ( $t_2$ ) and then a third spin (isospin)  $s = 1/2$  ( $t = 1/2$ ) to total spin  $S$  (isospin  $T$ ). In Eq. (14),  $\mathcal{A}$  stands for the operator that antisymmetrizes the three-particle wavefunction. Details on the construction of a fully antisymmetrized basis can be found in Ref. [21]. The basis states thus constructed are eigenstates of the unperturbed Hamiltonian  $H_0$  with  $N_3 = 2(n_1 + n_2) + l_1 + l_2$ .

In the conventional NCSM approach, it is customary to choose the truncation in the two-body system so that the many-body space is the minimal required to include completely the two-body space. For example, if we consider just  $S$ -wave interactions,  $N_2^{max} = N_3^{max}$  when one describes positive-parity states. However, one has to consider that the renormalization of the two-body system means that states lying above the cutoff  $N_2^{max}$  have been “integrated out” rather than simply discarded. Their effects are, thus, included implicitly in the effective two-body interaction. When these two interacting particles are embedded in a system with a larger number of particles, the spectators will carry energies associated with the HO levels they occupy. For example, of the  $(N_3 + 3)\omega$  total energy of one of the basis states (14),  $(2n_2 + l_2 + 3/2)\omega$  is carried by the relative motion of the spectator. As a consequence, the maximum energy available to the two-body subsystem is smaller than that allowed by the three-body cutoff  $N_3^{max}$  and some of the states removed by the truncation will not be accounted for by the renormalization. In order to account for all the two-body physics beyond our cutoff, we simply decouple the cutoff of the many-body problem from that of the subcluster defining any interaction. Each of our calculations is characterized by two cutoff parameters:  $N_2^{max}$  for the two-body subsystem, and  $N_3^{max}$  for the three-body system. For fixed  $N_2^{max}$  and  $N_3^{max}$ , we calculate the three-body energies  $E_{3;n}$ . We first increase  $N_3^{max}$  till convergence, which to a good approximation happens already when  $N_3^{max}$  is a couple of units larger than  $N_2^{max}$ , and we then increase  $N_2^{max}$ . We have shown in a previous publication [11] that proceeding this way greatly improves the convergence of the energies of a two-state-fermion system.

In the rest of this paper, we illustrate the application of our formalism to nucleons in the two channels with  $T = 1/2$ :  $J^\pi = 1/2^+, 3/2^+$ . These are the most interesting channels, since they are accessible in nucleon-deuteron scattering.

The energy in the trap should approach the energy of the untrapped system when the HO trap is weak, *i.e.*, for small values of  $\omega$ . The ground state in the  $T = 1/2, J^\pi = 1/2^+$  channel becomes the triton ( ${}^3\text{H}$ ) at an energy  $E_t = -8.482$  MeV [22], while all other states coalesce into the continuum states. Some of these states correspond to the  $S$ -wave scattering of a neutron on the deuteron, which can form inside the trap in the  $T = 1/2$  channels. We can then extract the  $nd$  phase shifts from the three-nucleon energies above the deuteron ground

state,  $E_{3;n} - E_d$ , with a relation similar to Eq. (12),

$$\frac{\Gamma(3/4 - (E_{3;n} - E_d)/2\omega)}{\Gamma(1/4 - (E_{3;n} - E_d)/2\omega)} = -\sqrt{(E_{3;n} - E_d)/2\omega} \cot \delta_3 \left( \sqrt{2\mu_{nd}(E_{3;n} - E_d)} \right), \quad (15)$$

where  $\mu_{nd}$  is the neutron-deuteron reduced mass, and the phase shift  $\delta_3(k)$  is given by an ERE expansion,

$$k \cot \delta_3(k) = -\frac{1}{a_3} + \frac{r_3}{2}k^2 + \dots \quad (16)$$

in terms of  $nd$  ERE parameters  $a_3$ ,  $r_3$ , *etc.* In the  $S = 3/2$  and  $S = 1/2$  channels the experimental values [23] of the scattering lengths are  $a_{3q} = 6.35 \pm 0.02$  fm and  $a_{3d} = 0.65 \pm 0.04$  fm, respectively.

It is important to note that Eq. (15) holds as long as the range of the  $nd$  interaction is much smaller than the effective trapping length  $b' = 1/\sqrt{\mu_{nd}\omega}$ . This makes high-cutoff calculations challenging since the  $nd$  size is rather large, of the order of the triplet two-nucleon scattering length. In the two-state fermion case we did succeed in extracting the atom-dimer scattering length using this method [11].

#### A. The channel $T = 1/2$ , $J^\pi = 3/2^+$

We first consider the case of three nucleons with  $T = 1/2$  coupled to  $J^\pi = 3/2^+$ . In this channel the three-nucleon force appears only in higher orders than included here, so the properties of the three-nucleon system are determined by the two-nucleon input. This situation is the same as for three two-state fermions [9, 11].

We start by discussing the convergence of the energy levels. For illustration, we take the ground state at a relatively large frequency  $\omega = 3$  MeV, but qualitative features are the same for other states and frequencies. We show LO and NLO results in Fig. 6 for various values of the two-body model space size  $N_2^{max}$ . For each  $N_2^{max}$ , the three-body model-space size defined by  $N_3^{max}$  is increased. There is a sharp decrease of the energy as  $N_3^{max} = N_2^{max} + 2$  and, as  $N_3^{max}$  increases further, the ground-state energy reaches a converged value. More precisely, as  $N_3^{max}$  increases, the energy changes by less than 0.1 keV for the values considered here. Thus faster convergence is obtained for a given  $N_2^{max}$  by increasing  $N_3^{max}$  beyond  $N_2^{max}$ , as observed before in the case of two-state fermions [11]. This can be seen for instance by comparing the LO energy obtained for  $N_2^{max} = 8$  and  $N_3^{max} = 10$ , which is  $E_3^{LO} = 7.058$  MeV, and the LO energy for  $N_2^{max} = N_3^{max} = 12$ , which is  $E_3^{LO} = 7.173$  MeV and further away from the extrapolated value  $E_3^{LO}(\infty)$  obtained from Eq. (17) below.

Figure 7 shows the convergence with respect to  $N_2^{max}$ . Clearly the energy converges to a finite value as the two-body cutoff increases. We can thus confirm that, as in the free-space case [6], no three-nucleon force is needed at these orders to renormalize the three-nucleon system. We can fit the cutoff dependence of the energy with

$$E_3(N_2^{max}) = E_3(\infty) + \frac{\epsilon_1}{(N_2^{max} + 3/2)^{1/2}} + \frac{\epsilon_3}{(N_2^{max} + 3/2)^{3/2}}, \quad (17)$$

where  $E_3(\infty)$  is the asymptotic value and  $\epsilon_{1,3}$  give the rate of convergence. The fits are performed for  $N_2^{max} \geq 12$ . At LO we obtain  $\epsilon_1^{LO} = 2.270$  MeV,  $\epsilon_3^{LO} = 1.676$  MeV, and  $E_3^{LO}(\infty) = 6.241$  MeV, which is  $\sim 500$  keV below the value obtained with the largest

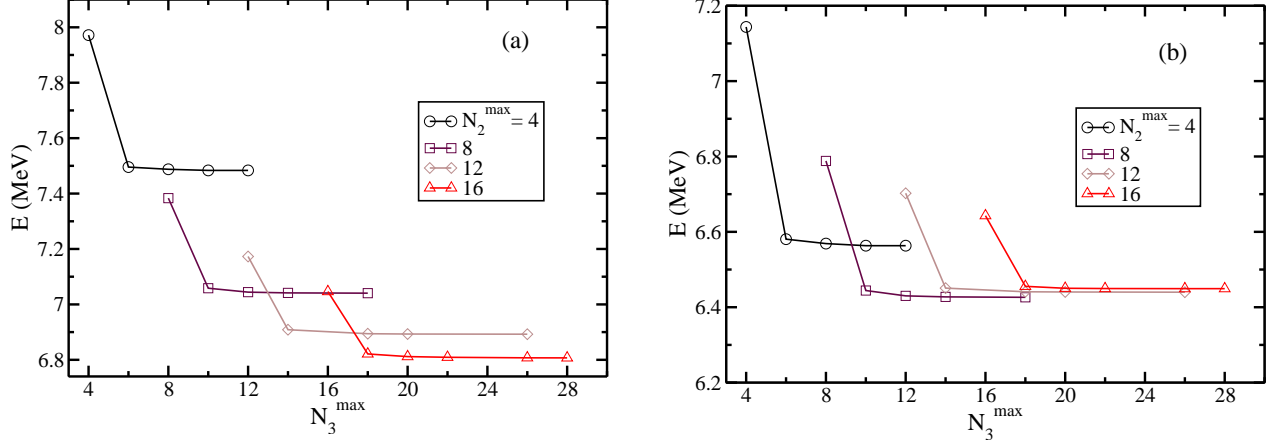


FIG. 6: (Color online) Ground-state energy of the trapped three-nucleon system coupled to  $T = 1/2$ ,  $J^\pi = 3/2^+$  as function of the three-body model-space size  $N_3^{\max}$ , for  $\omega = 3$  MeV: (a) LO; (b) NLO. Results are shown for different values of the two-body model-space size  $N_2^{\max}$ .

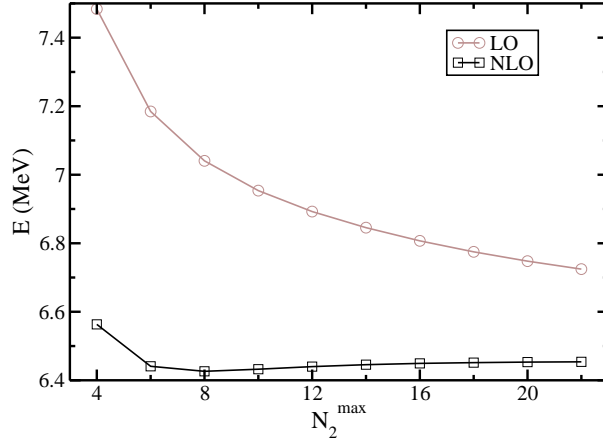


FIG. 7: (Color online) Ground-state energy of the trapped three-nucleon system coupled to  $T = 1/2$ ,  $J^\pi = 3/2^+$  as a function of  $N_2^{\max}$ , for  $\omega = 3$  MeV: LO (circles) and NLO (squares).

considered cutoff,  $N_2^{\max} = 22$ . At NLO, one obtains instead  $\epsilon_1^{NLO} = 0.3$  MeV,  $\epsilon_3^{NLO} = -2.99$  MeV, and  $E_3^{NLO}(\infty) = 6.417$  MeV, which is only  $\sim 40$  keV above the value obtained at  $N_2^{\max} = 22$ . The convergence at NLO is faster than that at LO, as can be seen in Fig. 7 and in the decrease of the coefficient  $\epsilon_1$  of the leading cutoff error. Although the specific numbers above depend strongly on  $\omega$ , the convergence pattern is qualitatively the same for other values of  $\omega$ .

For  $\omega = 1$  MeV, the first few eigenstates characterized by  $J^\pi = 3/2^+$  and  $T = 1/2$  are shown in Fig. 8. Since there is no free-space three-nucleon bound state in this channel, the lowest eigenstates of Eq. (2) for a weak trap correspond to “discretized”  $nd$  scattering states confined within the trap. For  $nd$  scattering in a  $S$  wave, we can select the lowest eigenstates with the configuration of orbital angular momentum  $L = 0$  and spin  $S = 3/2$ , where the two-nucleon interaction in the  $^1S_0$  channel does not play any role.

From the lowest energies of the eigenstates of the Hamiltonian (2) in the  $L = 0$ ,  $S = 3/2$  configuration we extract the  $S$ -wave  $nd$  phase shifts using Eq. (15). In Fig. 9 we show

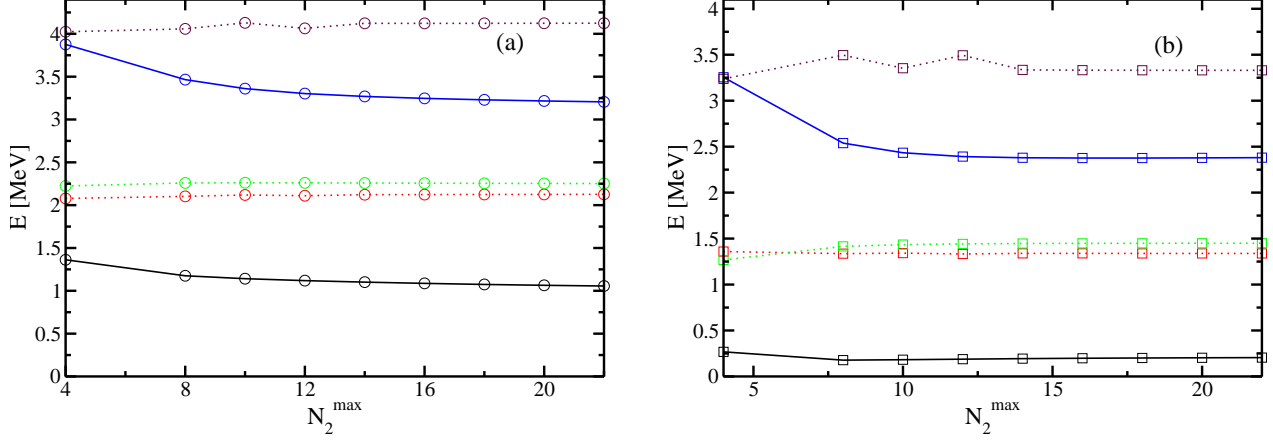


FIG. 8: (Color online) Lowest energies of the trapped three-nucleon system with  $T = 1/2$ ,  $J^\pi = 3/2^+$  as a function of  $N_2^{max}$ , for  $\omega = 1$  MeV: (a) LO; (b) NLO. The ground state and the third excited state (full lines) correspond to neutron-deuteron scattering within the trap in the  $L = 0$ ,  $S = 3/2$  channel, whereas the other states shown correspond to different  $L$ ,  $S$  configurations.

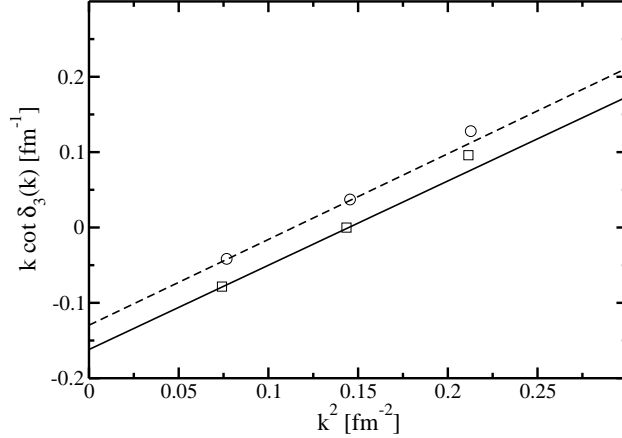


FIG. 9:  $k \cot \delta_3(k)$  in the  $T = 1/2$ ,  $L = 0$ ,  $S = 3/2$  channel obtained from the lowest energies at LO (circles) and NLO (squares) as a function of  $k^2$ , for  $\omega = 1$  MeV and  $N_2^{max} = 18$ . The dashed (full) line corresponds to a LO (NLO) linear fit to the two lowest energies.

$k \cot \delta_3(k)$  for  $\omega = 1$  MeV and  $N_2^{max} = 18$ . We extract the value of the quartet scattering length  $a_{3q}$  using Eq. (16). From the two lowest energies we obtain:  $a_{3q}^{LO} = 7.71$  fm and  $a_{3q}^{NLO} = 6.30$  fm. Note that by considering the second and third phase-shift points in Fig. 9 we would get instead:  $a_{3q}^{LO} = 6.29$  fm and  $a_{3q}^{NLO} = 4.92$  fm, which shows that higher-order ERE terms are more important at higher energy.

We now consider the procedure to extract  $a_{3q}$  for different values of the two-body cutoff and HO frequency. Extracted values of  $a_{3q}$  at LO and NLO as a function of the two-body cutoff are shown in Fig. 10 for  $\omega = 1$  MeV. At a fixed  $\omega$ , the scattering length  $a_{3q}$  should converge as the two-body cutoff is increased (since the energies of the three-nucleon system converge). For each  $\omega$ , we perform extrapolations to obtain the value  $a_{3q}(\infty)$  which would

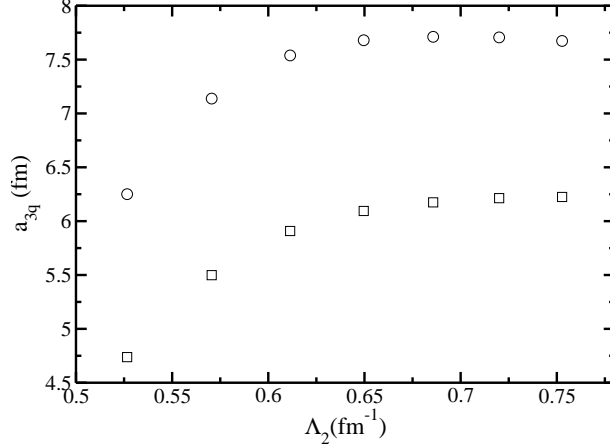


FIG. 10: Scattering length  $a_{3q}$  extracted from the spectrum of the trapped three-nucleon system in the channel  $T = 1/2$ ,  $L = 0$ ,  $S = 3/2$  as function of the cutoff  $\Lambda_2$ , for  $\omega = 1$  MeV: LO (circles) and NLO (squares).

correspond to  $\Lambda_2 \rightarrow \infty$ . We use for this purpose the trial function

$$\frac{1}{a_{3q}} = \frac{1}{a_{3q}(\infty)} + \frac{\alpha_1}{\Lambda_2^{p_1}} + \frac{\alpha_2}{\Lambda_2^{p_2}}, \quad (18)$$

where  $p_{1,2}$  and  $\alpha_{1,2}$  are parameters, which we fit to the six values of the scattering length obtained at the largest cutoffs.

Results of the extrapolation can be seen in Fig. 11, where  $a_{3q}(\infty)$  is plotted as a function of  $\omega$ . For HO frequencies from about 0.4 MeV to about 2 MeV the scattering length is such that  $7.30 \text{ fm} \leq a_{3q}^{LO}(\infty) \leq 7.53 \text{ fm}$  and  $6.08 \text{ fm} \leq a_{3q}^{NLO}(\infty) \leq 6.16 \text{ fm}$  for the trial function (18). Had we used a different trial function with fewer parameters, such as for instance the function (18) with  $\alpha_2 = 0$ , we would have obtained  $7.71 \text{ fm} \leq a_{3q}^{LO}(\infty) \leq 7.88 \text{ fm}$  and  $6.20 \text{ fm} \leq a_{3q}^{NLO}(\infty) \leq 6.24 \text{ fm}$ . While for larger traps we are closer to the continuum limit, our error in the scattering length increases. First, as  $\omega$  gets smaller, the imprecision on the value of  $a_{3q}$  stemming from the imprecision of the energy (*i.e.*, the difference between the values for finite  $N_2^{max}$  and  $N_2^{max} \rightarrow \infty$ ) are enhanced. This can be understood by noticing that in Eq. (15) the energy appears with  $\omega$  in the denominator. Second, numerical imprecision also arises as  $\omega$  gets smaller since the extrapolation to  $a_{3q}(\infty)$  is performed in these cases from data at lower  $\Lambda_2$ . Nevertheless we see a kind of plateau in the value of  $a_{3q}(\infty)$  for small  $\omega$ . With all imprecisions taken into account we can conclude that the results at NLO are in good agreement with the experimental value  $a_{3q} = 6.35 \pm 0.02 \text{ fm}$  [23] and with previous EFT calculations [6].

It might seem more natural to extract the scattering length directly from the extrapolated energies  $E_3(\infty)$  obtained in the fit (17). After having tried this method, we concluded that it could not give meaningful results: the behavior of  $a_{3q}$  as a function of  $\omega$  looked completely random. We believe that this is due to the fact that the extrapolated energies are not precise enough, because  $a_{3q}$  is strongly dependent on the input energies.



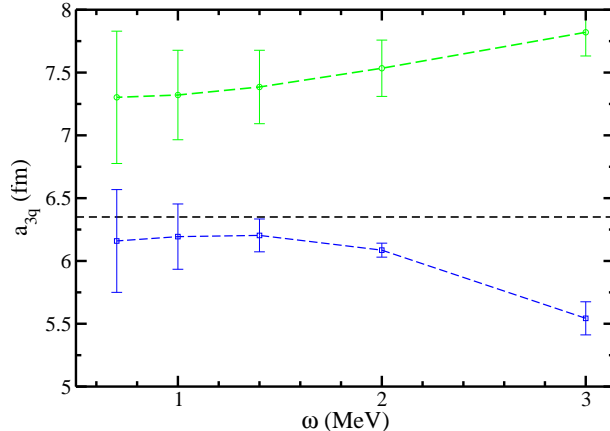


FIG. 11: (Color online) Extrapolated values  $a_{3q}(\infty)$  of the quartet scattering length for different values of  $\omega$ : LO (circles) and NLO (squares). The error bars correspond to the standard error obtained using the software Gnuplot. The horizontal dotted line marks the experimental value [23].

### B. The channel $T = 1/2$ , $J^\pi = 1/2^+$

We now consider the case of three nucleons with  $T = 1/2$  and orbital angular momentum and spins coupled to total angular momentum  $J^\pi = 1/2^+$ , the triton channel. The calculation proceeds along the same lines discussed in detail in the previous subsection, except for the role played by the three-body force, which is similar to that for three bosons [12].

The non-derivative three-nucleon potential (13) contributes in this channel and is known to be necessary for RG invariance at LO, at least in free space [7]. Since renormalization concerns UV momenta, it is not expected to be affected by the trap. We have confirmed this fact by examining the ground state of the three-nucleon system at various values of  $\omega$  in a calculation at LO but *without* a three-nucleon force. As before, for a fixed two-body cutoff  $\Lambda_2$  we increase the three-body model space until convergence is reached. Figure 12 shows the ground-state energy as a function of  $\Lambda_2^2/m_N$ . We can clearly see that as  $\Lambda_2$  increases, the ground-state energy decreases roughly linearly. Results for different values of  $\omega$  but the same two-body cutoff  $\Lambda_2$  are close to each other, which is a sign of the fact that the short-range two-nucleon interaction is much stronger than the long-range HO potential. This illustrates the collapse of the three-nucleon system in this channel when only a two-nucleon force is included in the pionless EFT [7].

Such a dramatic cutoff dependence shows that short-distance physics has not been accounted for properly. Renormalization can be achieved by including the non-derivative three-nucleon potential in Eq. (13) already at LO. We choose to determine the coefficient  $D_0$  so that the lowest energy of the three nucleons in the trap is fixed at the experimental value of the triton binding energy,  $E_t = -8.482$  MeV. It is convenient to introduce a cutoff  $N_3^{cut}$  above which the three-nucleon force is switched off. This means that the three-body force does not play a role for configurations with  $N_3 > N_3^{cut}$ . Nevertheless,  $D_0$  depends on both  $N_3^{cut}$  and  $N_3^{max}$  just as the energy obtained with only the two-nucleon force depends on  $N_3^{max}$  before convergence is reached. We take  $N_3^{cut} = N_2^{max}$ , and for each  $N_2^{max}$ ,  $D_0$  is adjusted to the triton binding energy. For large enough  $N_3^{max}$ , the three-body force becomes

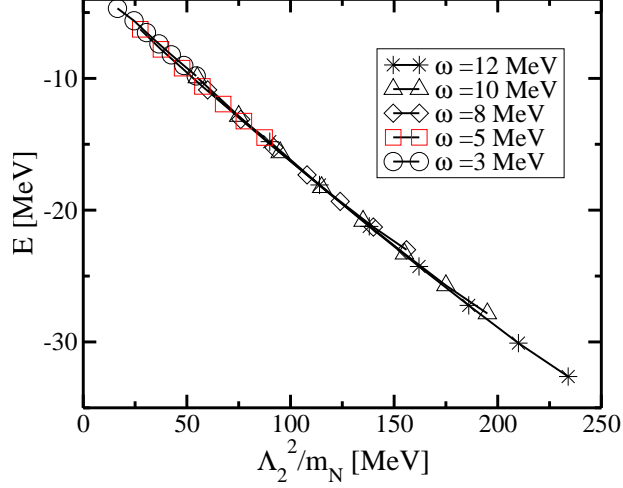


FIG. 12: (Color online) Ground-state energy of the trapped three-nucleon system with  $T = 1/2$  and  $J^\pi = 1/2^+$  as a function of  $\Lambda_2^2/m_N$ , for different frequencies  $\omega$ . Calculations are performed at LO but *without* a three-nucleon force.

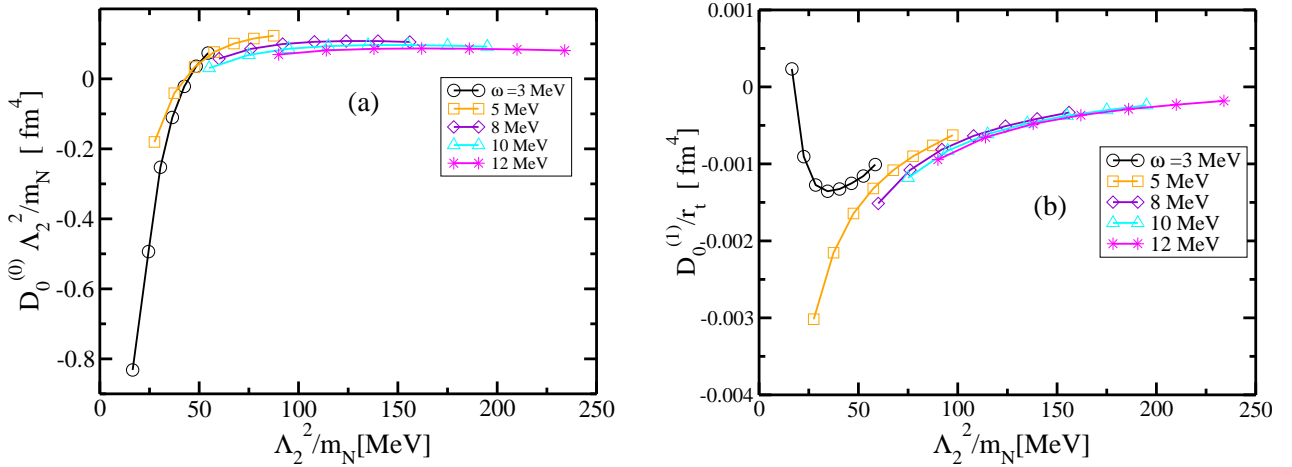


FIG. 13: (Color online) Three-nucleon coupling constants as function of  $\Lambda_2^2/m_N$ , for different values of  $\omega$ :  $D_0^{(0)}\Lambda_2^2/m_N$  (left panel) and  $D_0^{(1)}/r_t$  (right panel).

independent on  $N_3^{max}$ ,

$$D_0(N_3^{cut}, N_3^{max}) \rightarrow D_0(N_3^{cut}). \quad (19)$$

We again split the running of  $D_0(N_2^{max})$  into the various orders,  $D_0(\Lambda_2) = D_0^{(0)}(\Lambda_2) + D_0^{(1)}(\Lambda_2) + \dots$ . The running of  $D_0^{(0)}(\Lambda_2)$  and  $D_0^{(1)}(\Lambda_2)$  are shown in Fig. 13 for different values of  $\omega$ . The LO three-nucleon force becomes repulsive for  $\Lambda_2 \gtrsim 220$  MeV. We expect to see a limit cycle [7] in the behavior of the coupling  $D_0^{(0)}\Lambda_2^2$  as a function of  $\Lambda_2$ . However, the maximum cutoff we were able to consider here ( $\Lambda_2^2/m_N \sim 230$  MeV) is only approximately half the value where the second branch of the limit cycle appears [7].

Figure 14 shows the LO and NLO energies of the first three states in a trap with  $\omega = 5$  MeV. While the ground state is fixed at the experimental value of the triton binding energy, the other states converge to positive energy values, as befits continuum states in free space.

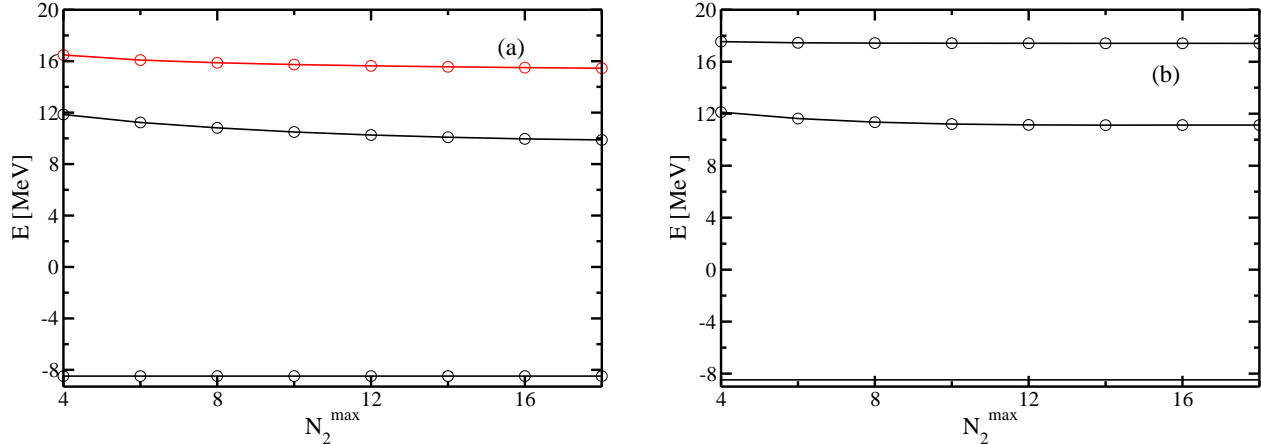


FIG. 14: (Color online) Energies of the ground state and first two excited states for the three-nucleon system coupled to  $T = 1/2$ ,  $J^\pi = 1/2^+$  as a function of the two-body model-space size  $N_2^{max}$ , for  $\omega = 5$  MeV: LO (left panel) and NLO (right panel). The three-body force is adjusted such that the ground state is fixed at the experimental value of the triton binding energy [22].

Again, results are similar for other HO frequencies.

From the scattering states we can again attempt to extract the  $S$ -wave  $nd$  phase shifts using Eq. (15). The result is shown in Fig. 15 for  $\omega = 1$  MeV and  $N_2^{max} = 18$ . By fitting the  $k \cot \delta_3(k)$  with a first-degree polynomial in  $k^2$ , as in Sec. IV A, we can extract the doublet scattering length  $a_{3d}$  using the two lowest energies. We then obtain  $a_{3d}^{LO} = 3.66$  fm and  $a_{3d}^{NLO} = 2.66$  fm. This is far larger than the experimental value  $a_{3d} = 0.65 \pm 0.04$  fm [23] and results obtained with pionless EFT in the continuum [7]. On the other hand, using the second and third values of the phase shift gives much smaller values for the scattering length,  $a_{3d}^{LO} = 0.319$  fm and  $a_{3d}^{NLO} = 0.281$  fm. Contrary to the quartet channel, the values for  $a_{3d}$  depend *strongly* on which energies they are extracted from. Possibly the energies considered here are not small enough to prevent higher-order ERE terms from spoiling the extraction of  $a_{3d}$ . This would explain why the third values of the phase shift in Fig. 15 is far away, at both LO and NLO, from the fit of  $k \cot \delta_3(k)$  obtained from the two lowest energies. A solution to overcome this problem would be to use larger computer resources to perform calculations at very low values of  $\omega$  but large values of  $N_2^{max}$ , and thus obtain better converged results at small enough energies.

## V. CONCLUSIONS AND OUTLOOK

We have presented an extension to nucleons of the work in Refs. [3, 9–12], in which the inter-particle interactions in a harmonic-oscillator basis are constructed within an EFT framework, by trapping the system in a HO potential. This approach is designed to improve upon the work of Ref. [2] by using a procedure to fix the two-body parameters from the two-body data, and thus more efficiently going beyond leading order. We considered explicitly here interactions up to NLO.

We have illustrated in the two-nucleon system the renormalization procedure developed in Refs. [3, 9–12]. We noted that the scattering properties can be recovered from the discrete spectra, as long as the trap length parameter  $b$  is much larger than the range of the interaction. As in the continuum, we were able to demonstrate systematic improvement of

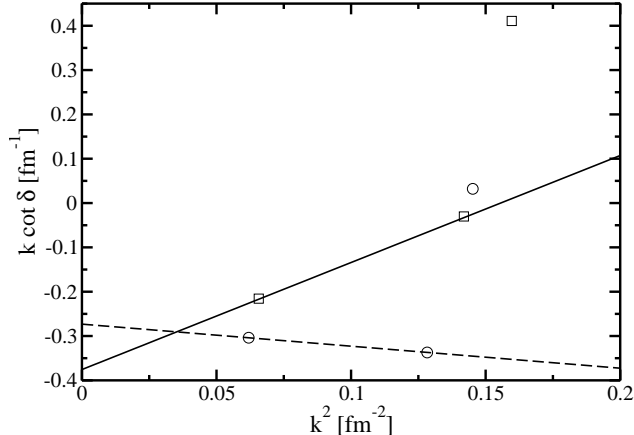


FIG. 15:  $k \cot \delta_3(k)$  in the  $L = 0$ ,  $S = 1/2$  channel obtained from the lowest energies at LO (circles) and NLO (squares) as a function of  $k^2$ , for  $\omega = 1$  MeV and  $N_2^{max} = 18$ . The dashed (full) line corresponds to a LO (NLO) linear fit to the two lowest energies.

observables order by order.

In the three-nucleon system, we showed the extent to which scattering information can be recovered from the discrete levels of the trap. We have presented results for the  $T = 1/2$ ,  $J^\pi = 3/2^+$  channel, where we have shown that, as in free space, no three-nucleon interaction is needed to renormalize the system at LO and NLO. We have estimated the quartet scattering length for nucleon-deuteron scattering. Results at NLO are in good agreement with the experimental value and previous EFT calculations. We also showed the collapse of the system in the  $T = 1/2$ ,  $J^\pi = 1/2^+$  channel when no three-nucleon force is included. This work opens the door for further development in describing scattering processes from bound-state physics, providing an alternative to other methods under development [24].

For the future, we plan to extend this work to  $^4\text{He}$  and  $^6\text{Li}$ , in order to test whether the reasonable agreement with experiment found in Ref. [2] was accidental or can be improved at NLO, thus testing the limits of the pionless EFT with increasing the number of nucleons. There is evidence [8], obtained with other methods, that the pionless EFT can, surprisingly, describe more tightly bound nuclei, like  $^4\text{He}$ , with parameters determined in the two- and three-nucleon systems. If this is indeed the case, this EFT could serve as the basis for more extensive nuclear-structure calculations. In addition, we intend to apply our method to the EFT in which the pion degrees of freedom are introduced explicitly, which should increase the reach of nuclear EFT.

## Acknowledgments

UvK thanks Hans Hammer for useful discussions. We are thankful to South Africa's National Institute for Theoretical Physics (NITheP) in Stellenbosch for hospitality during part of this work. This research was supported by the US NSF under grant PHY-0854912 (B.R.B. and J.R.); the US DOE under grants DE-FG02-97ER41014 (I.S.), DE-FC02-07ER41457 (I.S.), and DE-FG02-04ER41338 (J.R. and U.v.K.); and by the European Research Council

- [1] P. Navrátil, J.P. Vary, and B.R. Barrett, Phys. Rev. Lett. **84** (2000) 5728; Phys. Rev. C **62** (2000) 054311; P. Navrátil, S. Quaglioni, I. Stetcu, and B.R. Barrett, J. Phys. G **36** (2009) 083101.
- [2] I. Stetcu, B.R. Barrett, and U. van Kolck, Phys. Lett. B **653** (2007) 358.
- [3] I. Stetcu, J. Rotureau, B.R. Barrett, and U. van Kolck, J. Phys. G **37** (2010) 064033.
- [4] P.F. Bedaque and U. van Kolck, Ann. Rev. Nucl. Part. Sci. **52** (2002) 339.
- [5] U. van Kolck, hep-ph/9711222, in A. Bernstein, D. Drechsel, and T. Walcher (eds.), Proceedings of the Workshop on Chiral Dynamics 1997, Theory and Experiment, Springer-Verlag, Berlin, 1998; Nucl. Phys. A **645** (1999) 273; D.B. Kaplan, M.J. Savage, and M.B. Wise, Phys. Lett. B **424** (1998) 390; J. Gegelia, nucl-th/9802038; J.-W. Chen, G. Rupak, and M.J. Savage, Nucl. Phys. A **653** (1999) 386; D.R. Phillips, G. Rupak, and M.J. Savage, Phys. Lett. B **473** (2000) 209.
- [6] P.F. Bedaque and U. van Kolck, Phys. Lett. B **428** (1998) 221; P.F. Bedaque, H.-W. Hammer, and U. van Kolck, Phys. Rev. C **58** (1998) R641; F. Gabbiani, P.F. Bedaque, and H.W. Griesshammer, Nucl. Phys. A **675** (2000) 601; M.C. Birse, nucl-th/0509031.
- [7] P.F. Bedaque, H.-W. Hammer, and U. van Kolck, Nucl. Phys. A **676** (2000) 357; H.-W. Hammer and T. Mehen, Phys. Lett. B **516** (2001) 353; P.F. Bedaque, G. Rupak, H.W. Griesshammer, and H.-W. Hammer, Nucl. Phys. A **714** (2003) 589; H.W. Griesshammer, Nucl. Phys. A **744** (2004) 192; Nucl. Phys. A **760** (2005) 110; Few-Body Syst. **38** (2006) 67; I.R. Afnan and D.R. Phillips, Phys. Rev. C **69** (2004) 034010; T. Barford and M.C. Birse, J. Phys. A **38** (2005) 697; L. Platter, Phys. Rev. C **74** (2006) 037001.
- [8] L. Platter, H.-W. Hammer, and U.-G. Meißner, Phys. Lett. B **607** (2005) 254; J. Kirscher, H.W. Griesshammer, D. Shukla, and H.M. Hofmann, Eur. Phys. J. A **44** (2010) 239.
- [9] I. Stetcu, B.R. Barrett, U. van Kolck, and J.P. Vary, Phys. Rev. A **76** (2007) 063613.
- [10] I. Stetcu, J. Rotureau, B.R. Barrett, and U. van Kolck, Ann. Phys. **325** (2010) 1644.
- [11] J. Rotureau, I. Stetcu, B.R. Barrett, M.C. Birse, and U. van Kolck, Phys. Rev. A **82** (2010) 032711.
- [12] S. Tölle, H.-W. Hammer, and B.C. Metsch, Comptes Rendus Physique **12** (2011) 59.
- [13] T. Luu, M.J. Savage, A. Schwenk, and J.P. Vary, Phys. Rev. C **82** (2010) 034003.
- [14] P.F. Bedaque, H.-W. Hammer, and U. van Kolck, Phys. Rev. Lett. **82** (1999) 463; Nucl. Phys. A **646** (1999) 444; R.F. Mohr, R.J. Furnstahl, R.J. Perry, K.G. Wilson, and H.-W. Hammer, Ann. Phys. **321** (2006) 225; L. Platter and D.R. Phillips, Few-Body Syst. **40** (2006) 35.
- [15] H.A. Bethe, Phys. Rev. **76** (1949) 021603.
- [16] J.J. de Swart, C.P.F. Terheggen, and V.G.J. Stoks, nucl-th/9509032; D.E. Gonzalez Trotter *et al.*, Phys. Rev. Lett. **83** (1999) 409.
- [17] T. Busch, B.-G. Englert, K. Rzażewski, and M. Wilkens, Found. Phys. **28** (1998) 549; S. Jonsell, Few-Body Syst. **31** (2002) 255; D. Blume and C.H. Greene, Phys. Rev. A **65** (2002) 043613; M. Block and M. Holthaus, Phys. Rev. A **65** (2002) 052102; E.L. Bolda, E. Tiesinga, and P.S. Julienne, Phys. Rev. A **66** (2002) 013403; A. Bhattacharyya and T. Papenbrock, Phys. Rev. A **74** (2006) R041602.
- [18] E. Fermi, Ric. Scientifica **7** (1936) 13; G. Breit, Phys. Rev. **71** (1947) 215; K. Huang and C.N. Yang, Phys. Rev. **105** (1957) 767.

- [19] T. Mehen, Phys. Rev. A **78** (2008) 013614.
- [20] V.G.J. Stoks, R.A.M. Klomp, M.C.M. Rentmeester, and J.J. de Swart, Phys. Rev. C **48** (1993) 792.
- [21] P. Navrátil, G.P. Kamuntavičius, and B.R. Barrett, Phys. Rev. C **61** (2000) 044001.
- [22] J.E. Purcell, J.H. Kelley, E. Kwan, C.G. Sheu, and H.R. Weller, Nucl. Phys. A **848** (2010) 1.
- [23] W. Dilg, L. Koester, and W. Nistler, Phys. Lett. B **36** (1971) 208.
- [24] K.M. Nollett, S.C. Pieper, R.B. Wiringa, J. Carlson, and G.M. Hale, Phys. Rev. Lett. **99** (2007) 022502; S. Quaglioni and P. Navrátil, Phys. Rev. Lett. **101** (2008) 092501; Phys. Rev. C **79** (2009) 044606.